Elucidation of the physicochemical properties and potency of siRNA-loaded small-sized lipid nanoparticles for siRNA delivery

Yusuke Sato,†[a] Yusuke Note,†[a] Masatoshi Maeki,[b] Noritada Kaji,[cd] Yoshinobu Baba,[cd] Manabu Tokeshi,[bd] Hideyoshi Harashima⋆[a]

[a]*Faculty of Pharmaceutical Sciences, Hokkaido University, Kita 12 Nishi 6, Kita-ku, Sapporo 060-0812, Japan*

[b]*Division of Applied Chemistry, Faculty of Engineering, Hokkaido University, Kita 13 Nishi 8, Kita-ku, Sapporo 060-8628, Japan*

[c]*Department of Applied Chemistry, Graduate School of Engineering, Nagoya University, Furo-cho, Chikusa-ku, Nagoya 464-8603, Japan*

[d]*ImPACT Research Center for Advanced Nanobiodevices, Nagoya University, Furo-cho, Chikusa-ku, Nagoya 464-8603, Japan*

†These authors are contributed equally to this work.

⋆Corresponding author

Hideyoshi Harashima, PhD
Faculty of Pharmaceutical Science
Hokkaido University
Sapporo, Hokkaido, 050-0812, Japan.
Tel.: +81 11 706 3919
Fax: +81 11 706 3734
E-mail: harasima@pharm.hokudai.ac.jp

Abstract

Because nanoparticles with diameters less than 50 nm penetrate stromal-rich tumor tissues more efficiently, the synthesis of small-sized nanoparticles encapsulating short interfering RNA (siRNA) is important in terms of realizing novel siRNA medicine for the treatment of various cancers. Lipid nanoparticles (LNPs) are the leading systems for the delivery of siRNA *in vivo*. Limit size LNPs were successfully synthesized using a microfluidic mixing technique. However, the physicochemical properties and potential for *in vivo* siRNA delivery of the limit-size LNPs have not been examined in detail. In the present study, we prepared LNPs with different diameters from 32 to 67 nm using a microfluidic mixing devise and examined the physicochemical properties of the particles and the potential for their use in delivering siRNA *in vitro* and *in vivo* to liver. Reducing the size of the LNPs causes poor-packing and an increased surface area, which results in their instability in serum. Moreover, it was revealed that the ability of endosomal escape (cytosolic siRNA release) of the smaller LNPs are subject to inhibition by serum compared to that of larger counterparts. Taken together, an increase in packing and avoiding the adsorption of serum components are key strategies for the development of next-generation highly potent, small-sized LNPs.

Key words

Small-sized lipid nanoparticles, siRNA delivery, Microfluidic device, Protein adsorption, Stability, Endosomal escape

1. Introduction

Short interfering RNA (siRNA), which inhibits specific gene expression through RNA interference (RNAi), is expected to be a novel medicine for treating refractory diseases, including cancer. Due to the physicochemical properties of the siRNAs, which include a high molecular weight, anionic charge and hydrophilicity, a delivery system will be needed to deliver the siRNAs to the cytosol, which is the site of action. Typically, an efficient gene silencing can be obtained in *in vitro* cultured cells after the introduction of the siRNAs by using appropriate transfection reagents. However, although numerous siRNA delivery compounds have been developed, only a few formulations have reached the level of human clinical trials [1-3]. This rather disappointing situation comes from severe barriers in the living body and complicated interactions with biological components including serum proteins. Therefore, siRNA delivery systems need to have important properties such as stability in the blood circulation, avoiding recognition by the reticuloendothelial system, distribution to target tissues and cells, and endosomal escape for cytoplasmic delivery.

Because of the leaky vasculature and dysfunctional lymphatic drainage in tumor tissue, nanoparticles in the blood stream can accumulate in tumor tissues. This process, which is referred to the enhanced permeability and retention (EPR) effect, is an accepted strategy for targeting solid tumor tissue [4, 5]. Traditional polyethyleneglycol (PEG)-modified (pegylated) liposomal doxorubicin (Doxil®), which is 100 nm in diameter, accumulates in the stromal-poor tumor tissues at high levels, compared to free doxorubicin, and shows a better antitumor effect [6]. On the other hand, Doxil does not penetrate stromal-rich tumor tissue and accumulates only in the perivascular region [7, 8]. More importantly, the three Food and Drug Administration (FDA)-approved nanomedicines for cancer, including Doxil, only modestly improved the overall survival of patients [9]. It is known that a dense extracellular matrix such as collagen and hyarulonan function as physical barriers to the penetration of nanoparticles [7, 10, 11]. Recently, Cabral et al. clearly demonstrated that 30 nm-sized micelles penetrate poorly in permeable tumor tissues, but not 70 nm-sized counterparts [12]. Because siRNA cannot pass through cellular membranes, siRNA-loaded nanoparticles must penetrate permeable tumor tissue poorly and be taken up by tumor cells. Therefore, controlling the size of a nanoparticle to 30 nm is essential for realizing siRNA-based tumor therapeutics.

A bottom-up approach for preparing limit-size lipid nanoparticles (LNPs) using a microfluidic mixing was recently reported [13]. Using this approach, Belliveau et al. reported on the preparation of 30 nm-sized siRNA-loaded LNPs [14]. This technology

is expected to expand the possibility for realizing effective LNP-based siRNA medicine for the treatment of tumors. However, the physicochemical properties and potency of such small-sized LNPs have not been examined yet.

In the present study, we prepared a series of LNPs with different diameters, ranging from 32 to 67 nm using a microfluidic device with a staggered herringbone micromixer structure and examined the impact of LNP size on physicochemical properties and their potential for the delivery of siRNA. The findings indicate that downsizing the LNPs leads to a reduced gene silencing activity, which results from poor-packing and instability in the presence of serum and a lower endosomal escape ability. Since smaller LNPs showed a high gene silencing activity in the absence of serum, the absorption of serum components to the wide surface area of the small-sized LNPs would be expected to result in a reduced potency. We believe that these finding provide insights and opportunities for developing the siRNA-loaded, small-sized LNPs with a high gene silencing activity.

2. Materials and methods

2.1 Materials

A pH-sensitive cationic lipid, YSK05, was synthesized as described previously [15]. Cholesterol (chol) was purchased from SIGMA Aldrich (St. Louis, MO). 1,2-Dimirystoyl-*sn*-glycero, methoxyethyleneglycol 2000 ether (PEG-DMG), 1,2-dioleoyl-*sn*-glycero-3-phosphatidylcholine (DOPC), 1,2-dioleoyl-*sn*-glycero-3-phosphatidylserine (DOPS) and 1,2-dioleoyl-*sn*-glycero-3-phosphatidyethanolamine (DOPE) were purchased from the NOF Corporation (Tokyo, Japan). 1,2-Dioleoyl-*sn*-glycero-3-phosphoethanolamine-*N*-(7-nitro-2-1,3-benzoxadiazol-4-yl) (NBD-PE) and 1,2-dioleoyl-*sn*-glycero-3-phsphoethanolamine-*N*-(lissamine rhodamine B sulfonyl) (Rho-PE) were purchased from Avanti Polar Lipids (Alabaster, AL). 3,3′-Dioctadecyloxacarbocyanine perchlorate (DiO) and Ribogreen were purchased from Molecular Probes (Eugene, OR, USA). TNS was purchased from Wako Chemicals (Osaka, Japan). FITC-conjugated Isolectin B4 was purchased from Vector Laboratories (Burlingame, CA). The sequences for the sense and antisense strands of siRNAs used in this study are listed in Table S1.

2.2 Animals

ICR mice, 4 weeks old, were purchased from Japan SLC (Shizuoka, Japan). The experimental protocols were reviewed and approved by the Hokkaido University Animal Care Committee in accordance with the guidelines for the care and use of laboratory animals.

2.3 Fabrication of a microfluidic device

The microfluidic device was fabricated by using double-layered photolithography and replica-molding techniques. The master mold was made from SU-8 3050 (Nippon Kayaku Co., Ltd., Tokyo, Japan) that was formed into a 3-inch silicon wafer (SUMCO Co., Tokyo, Japan). The height of the 1st layer was 79 μm and that of the 2nd layer (for mixer structures) was 31 μm. The width of the microchannel was 200 μm. After fabrication of the SU-8 mold, the surface modification was conducted with 1 *H*, 1 *H*, 2 *H*, 2 *H*-perfluorooctyl-trichlorosilane (Sigma-Aldrich). Polydimethylsiloxane (PDMS) (SILPOT 184 W/C, Dow Corning Toray, Tokyo, Japan) was then poured onto the SU-8 mold, after which, it was cured at 70˚C. The PDMS replica was cut out from the SU-8 wafer and was bonded to a glass substrate by an oxygen plasma treatment. Poly (ethereetherketone) (PEEK) capillaries (Institute of Microchemical Technology Co.,

Ltd., Kanagawa, Japan,) (Inner diameter = 300 μm, outer diameter = 500 μm) were connected to the inlet and the outlet of the microfluidic device and the junction was sealed by superglue.

2.4 Preparation of LNPs

An ethanol solution containing YSK05, chol, and PEG-DMG at a molar ratio of 70/30/1-3 were prepared at a concentration of 8 mM total lipid. The siRNA was dissolved in 25 mM acetate buffer (pH4.0) at a concentration of 0.071 mg/mL. LNPs were prepared by mixing the lipids in ethanol and siRNA in an aqueous solution using the microfluidic mixer at a combined flow rate of 1.5 mL/min (0.375 mL/min for the lipid solution and 1.125 mL for the siRNA solution). Syringe pumps (Harvard apparatus, MA) were used to control the flow rate. The resulting LNP solution was then dialyzed for at least 2 hr against 20 mM MES buffer (pH 6.0) followed by an overnight dialysis against phosphate buffered saline (PBS) (pH7.4) using Spectra/Por 4 dialysis membranes (molecular weight cut-off 12,000-14,000 Da, Spectrum Laboratories, Rancho Dominguez, CA).

The size and ζ-potential of the LNPs were measured by a Zetasizer Nano ZS ZEN3600 instrument (Malvern Instruments, Worchestershire, UK). The encapsulation efficiency and total concentration of siRNA were measured by a Ribogreen assay as described previously [15]. The method used to measure the apparent pKa value of the LNPs involved a TNS assay as described previously [15]. The apparent pKa was determined as the pH giving rise to half-maximal fluorescent intensity. The percentage of cationically charged pH-sensitive cationic lipid was calculated using the Henderson-Hasselbalch equation.

2.5 Transmission electron microscopy analysis

A drop of an aqueous solution containing LNPs was absorbed to carbon-coated copper grids (400 mesh) and the samples was stained with a 2% phosphor tungstic acid solution (pH7.0) for 20 sec. The sample was observed by a transmission electron microscope (JEM-1400Plus, JEOL Ltd., Tokyo, Japan).

2.6 Measurement of total surface area of LNPs

Thirty μM of LNP lipid and 6 μM of TNS were mixed in 200 μL of 10 mM citrate, 10 mM sodium phosphate, 10 mM Tris-HCl and 120 mM NaCl at pH 8.50. Fluorescence was measured using a spectrofluorometer (Enspire, PerkinElmer, MA, USA) with settings of λ_{ex} = 321 nm, λ_{em} = 447 nm. Fluorescence of a control with no LNP lipid

was also measured as a blank. We used the following formula to calculate the theoretical total surface area of the 3%PEG-LNPs:

$$\text{Total surface area}\,(3\%\text{PEG}-\text{LNPs}) = \text{Total surface area}\,(1\%\text{PEG}-\text{LNPs}) \times \frac{\text{Diameter}\,(1\%\text{PEG}-\text{LNPs})}{\text{Diameter}\,(3\%\text{PEG}-\text{LNPs})}$$

The relative value of the total surface area of the 3%PEG-LNPs was calculated by applying 1 to the total surface area (1%PEG-LNPs).

2.7 Generalized polarization (GP) measurement

One mol% laurdan-labeled LNPs were diluted with PBS to a total lipid concentration of 0.5 mM. After pre-incubation at 37°C for 10 min, laurdan fluorescence was measured using a spectoflurometer (FP-6300, JASCO, Tokyo, Japan) at 37°C. the GP value was calculated from the emission spectra as follows:

$GP = (I_{440} - I_{490})/(I_{440}+I_{490})$

where I_{440} and I_{490} are the intensities at the emission maxima of 440 and 490 nm, respectively, using a fixed excitation wavelength of 340 nm.

2.8 Hemolysis assay

Fresh red blood cells (RBCs) were collected from an ICR mouse and suspended in a buffer (20 mM MES and 130 mM NaCl at pH 6.0). Plasma was obtained from the same mouse. The fixed concentration of the RBC suspension with various amounts of plasma was mixed with 50 μM of LNP lipid, and the suspension incubated at 37°C for 30 min. After the incubation, the absorbance at 545 nm of the supernatant was measured after centrifugation (4°C, 400 *g*, 5 min). The samples incubated with 0.5 wt/vol% TritonX-100 as appositive control and without LNPs as a negative control were also measured. The quantity of protein in the plasma was measured using a BCA protein assay kit (Pierce).

2.9 siRNA release assay

LNPs (1 mM lipid) suspended in PBS at pH 7.4 and FBS were mixed together at a volume ratio of 4:1. The mixture was incubated at 37°C for 20 min. Subsequently, anionic liposomes (DOPS:DOPC:DOPE:NBD-PE:Rho-PE at a molar ratio of 25:25:48:1:1) were added to the serum-LNP mixture at a cationic/anionic lipid molar ratio of 1.6 in 150 mM MES buffer at pH 6.0. As a control, the sample without anionic

liposomes was measured. The siRNA encapsulation rate of LNPs was measured by Ribogreen assay.

2.10 Fluorescent resonance energy transfer (FRET)

The LNPs encapsulating an equal molar amount of Cy3-labeled siRNA and Cy5-labeled siRNA were mixed with 10% FBS in PBS at pH7.4. Final siRNA concentration was fixed at 12.5 μg/mL. After incubation at 37℃ for each indicated time, fluorescence of Cy3 was measured using a spectoflurometer (FP-6300) with settings of λ_{ex} = 550 nm, λ_{em} = 568 nm. The sample containing 1 wt/vol% SDS was measured as a positive control.

2.11 Gene silencing activity *in vitro*

HeLa cells stably expressing Firefly and Renilla luciferase (HeLa-dluc) were cultured in cell-culture dishes (Corning) containing DMEM supplemented with 10% FBS, penicillin (100U/mL), streptomycin (100 mg/mL) and G418 (0.4 mg/mL) at 37℃ in 5% CO_2. HeLa-dluc cells were seeded at a density of 2-2.5×10^4 cells per well in 24-well plates in growth medium 24 hr prior to transfection and the resulting samples incubated overnight at 37℃ in 5% CO_2. For transfection, LNPs at the indicated concentrations of siGL4 were diluted with DMEM containing 10% FBS or serum free DMEM, and were added to cells after aspiration of the spent media. The LNPs were incubated for 3 hr with the cells, and new growth media was added after aspiration of the spent media, followed by a further incubation for 21 hr prior to an analysis for luciferase expression. Firefly and Renilla luciferase activities were analyzed using the Dual-Glo assay (Promega, WI, USA) according to manufacturer's protocol. Luminescence was measured using a luminometer (Luminescencer-PSN, ATTO, Tokyo, Japan). For data analysis, Firefly luciferase activity was normalized by Renilla luciferase activity, and the treated samples were compared with the untreated samples to calculate the efficiency of luciferase silencing.

2.12 Cellular uptake

Twenty-four hours prior to transfection, HeLa-dluc cells were seeded at a density of 1×10^5 cells per well in 6-well plates in growth medium and incubated overnight at 37℃ in 5% CO_2. For transfection, the LNPs labeled with both DiO (0.5 mol% of total lipid) and Cy5-siGFP (10 mol% of total siRNA) were diluted with DMEM containing 10% FBS or serum free DMEM at 30 nM siRNA, and was added to the cells after aspiration of the spent media. The LNPs were incubated with the cells for the indicated times. The

cells were washed with PBS twice and detached by treatment with a trypsin solution. The cells were resuspended with FACS buffer (PBS containing 0.5% bovine serum albumin and 0.02% sodium azide) after centrifugation (4℃, 400 *g*, 5 min) and aspiration of supernatant. The cells were filtered through a nylon mesh and measured by FACSCalibur (Becton Dickinson, Franklin Lakes, NJ, USA) and analyzed using Cell Quest software (Becton Dickinson, Franklin Lakes, NJ, USA). Correlation coefficient (R) was calculated from DiO/Cy5 dot-plots.

2.13 Measurement of plasma coagulation factor VII (FVII) activity

ICR mice were intravenously administered with the LNP formulating siFVII at the indicated dose. The mice were anesthetized after 24 hr after siRNA treatment, and blood was obtained by cardiac puncture and processed to plasma using heparin. Plasma FVII activity was measured using a Biophen FVII chromogenic assay kit (Aniara Corporation, West Chester, OH, USA) according to the manufacturer's protocol.

2.14 Observation of intrahepatic siRNA distribution

ICR mice were intravenously administered with Cy5-siGFP formulated in the LNPs at a dose of 0.5 mg/kg. Twenty-five minutes after administration, the mice were injected with FITC-conjugated Isolectin B4 (40 μg/mouse) and liver tissues were collected after a 5 minute incubation. Intrahepatic distribution of siRNA was observed using a Nikon A1 (Nikon Co. Ltd., Tokyo, Japan). Images were captured by ×60 objective.

2.15 Measurement of LNP concentration in blood

ICR mice were intravenously injected with DiD (1 mol% of total lipid) labeled LNPs at a dose of 1 mg/kg. Blood (24 mL per each time point) was collected from the tail vein after the indicated time points. The blood samples were diluted with 1% SDS solution, and fluorescence of DiD was measured using a spectrofluorometer (Enspire) with settings of λ_{ex} = 650 nm, λ_{em} = 680 nm. A standard curve was prepared for the LNP solution and the blood from untreated mice.

2.16 Statistical analysis

Results are expressed as mean±SD. Statistical comparisons between two groups were evaluated by Student's *t*-test and corrected by ANOVA for multiple comparisons.

3. Results

3.1 Characterization of LNPs synthesized by a microfluidic mixing

The LNPs used in this study were synthesized by the rapid mixing of an ethanolic lipid mixture and aqueous siRNAs using a microfluidic device with a staggered herringbone micromixer structure (Figure 1A). A microfluidic device with a staggered herringbone micromixer structure was used to produce turbulent flow and to achieve rapid mixing of the two solutions. The rapid mixing inhibits particle aggregation, the formation of heterogeneous and larger particles, and results in the formation of small-sized LNPs. As the LNPs contain a large proportion (70 mol%) of YSK05, which has a cone-shaped structure, their structure is estimated to contain a nanostructured core but not a lipid bilayer (envelope), like liposomes. Moreover, since the interfacial area of the PEG-DMG molecule is much higher than that of the main components of the LNP lipid, YSK05 and cholesterol, the amount of PEG-DMG should dominantly determine the size of the LNPs. To confirm this, 5 kinds of LNPs with various amounts of PEG-DMG were prepared. The size of the LNPs decreased from 67.1 to 37.3 nm increasing amount of PEG-DMG (1 to 3 mol% of total lipid) (Figure 1B). Moreover, transmission electron microscopic observations revealed that both 1%PEG- and 3%PEG-LNPs exhibited a nanostructured core (Figure 1C, D), which is similar to findings in a previous report [16, 17]. The 5 kinds of LNPs showed similar ζ-potentials (0 to 5 mV) at pH 7.4 (data not shown). The siRNA encapsulation efficiency was nearly 100% and was not dependent on the amount of PEG-DMG (Figure 1E). The apparent pKa value, which is known to be one of the most significant parameters in determining the efficiency of siRNA delivery to hepatocytes [1], of the 1%PEG-LNPs was slightly lower than that of the 3%PEG-LNPs (6.25 for 1%PEG-LNPs and 6.45 for 3%PEG-LNPs) (Figure 1F).

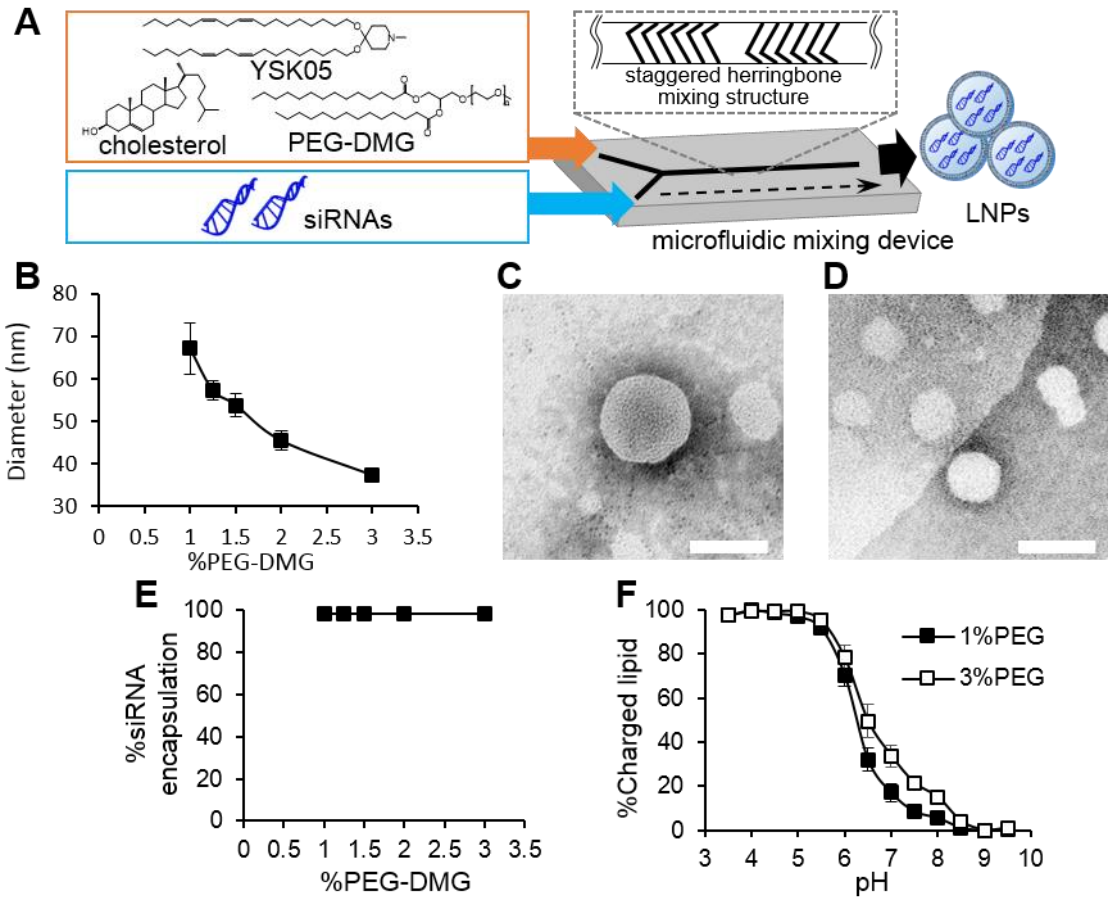

Figure 1. Characteristics of LNPs synthesized using a microfluidic mixing device. (A) Schematic illustration of the synthetic process of the LNPs. (B) Size of the LNPs containing different amount of PEG-DMG measured by dynamic light scattering. n=3. (C, D) Representative TEM micrograph of 1%PEG-LNPs (C) and 3%PEG-LNPs (D). Scale bars represent 50 nm. (E) Percentage of siRNA encapsulation measured by a Ribogreen assay. n=3. (F) Percentage of cationically charged lipids determined by a TNS assay. n=3. Data are represented as the mean±SD.

3.2 Impact of LNP size on *in vivo* hepatocellular siRNA delivery

In order to reveal the impact of particle size on the gene silencing activity *in vivo*, the FVII gene silencing activity of 1%PEG- and 3%PEG-LNPs was evaluated in mice. The 3%PEG-LNPs showed a significantly lower gene silencing activity with a median effective dose (ED_{50}) of 0.4 mg/kg compared to the 1%PEG-LNPs (ED_{50}: 0.1 mg/kg) (Figure 2A). Both the 1%PEG- and 3%PEG-LNPs were rapidly cleared (half-time: approximately 3 min) from the blood stream after an intravenous administration at a similar rate (Figure 2B). Next, microscopic observation of liver tissues was carried out

to evaluate both the accumulation and intrahepatic localization of siRNA. For the 1%PEG-LNPs, the siRNAs were homogenously localized to the extravascular region where hepatocytes are present, and also accumulated in blood vessels (Figure 2C, upper panels). This localization pattern is consistent with our previous findings on an LNP with similar lipid composition and particle size but with a different density of PEG-DMG [18]. On the other hand, for the 3%PEG-LNPs, most of the siRNAs can be found in extravascular region and only a few siRNA molecules accumulated in blood vessels (Figure 2C, lower panels). The hepatocellular siRNA localization of 3%PEG-LNPs had a punctuate pattern, which was different from 1%PEG-LNPs (a diffuse pattern) (Figure 2C). The amount of siRNA that accumulated in liver tissue appeared to be lower than that for the 1%PEG-LNPs (Figure 2C). To quantitatively determine the siRNAs delivered to liver tissues, Cy5 fluorescence in liver homogenates was measured and the results indicated that the amount of siRNAs delivered by 3%PEG-LNPs was significantly lower than that delivered by 1%PEG-LNPs (Figure S1). Therefore, the lower gene silencing activity of the 3%PEG-LNPs can be explained in part by a lower accumulation of siRNA in hepatocytes.

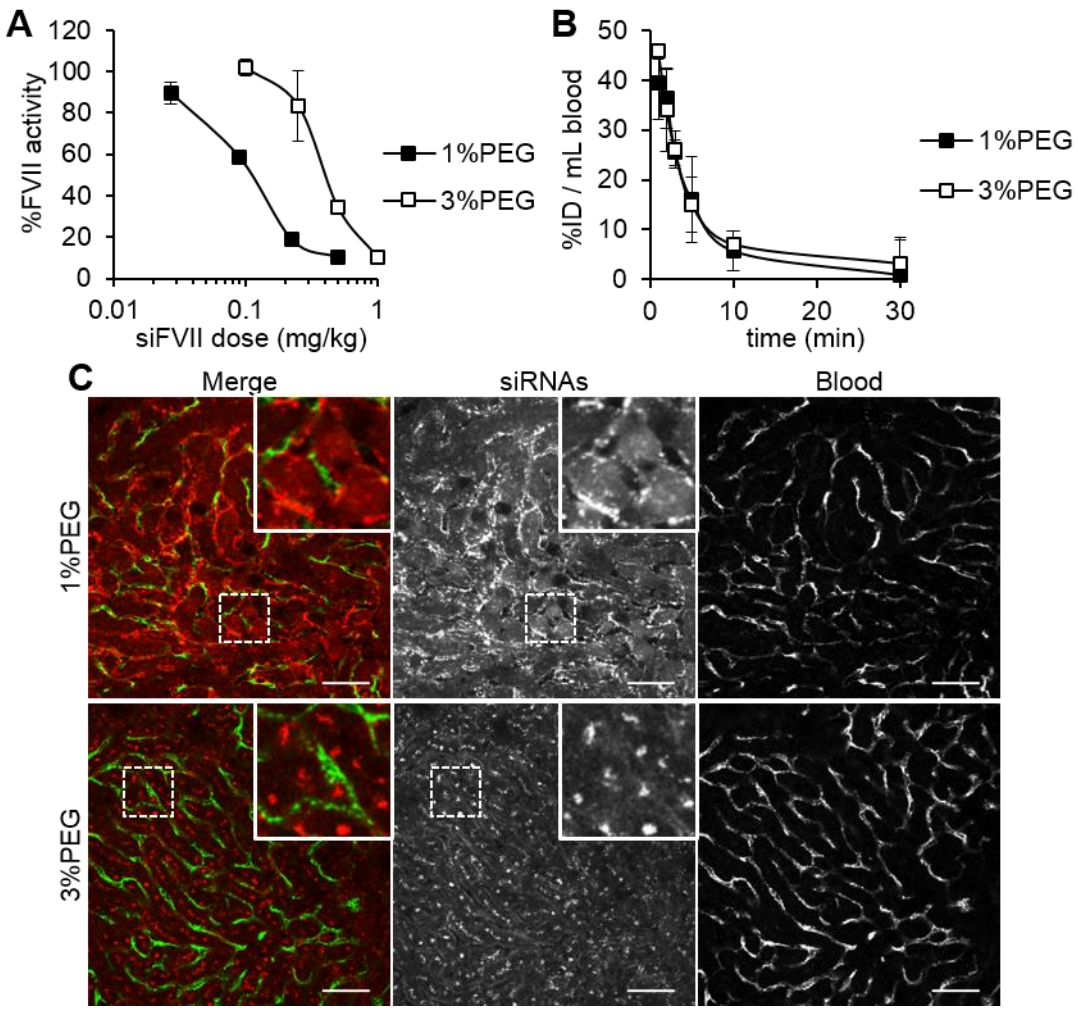

Figure 2. *In vivo* activity and biodistribution of 1%PEG-LNPs and 3%PEG-LNPs. (A) FVII gene silencing activity of the LNPs. n=3. (B) Blood concentration of the LNPs after intravenous administration. n=3. Data are represented as the mean±SD. (C) Intrahepatic distribution of siRNAs delivered by the LNPs. Blood vessels and siRNAs are visualized as green and red, respectively. Scale bars indicate 50 μm.

3.3 Impact of LNP size on *in vitro* siRNA delivery

In order to determine the impact of particle size on gene silencing activity in detail, the activity of 5 kinds of LNPs with different PEG-DMG contents was evaluated *in vitro*. In this experiment, the LNPs were added to HeLa-dluc cells in the presence or absence of serum in order to determine the effect of serum on gene silencing efficiency. In the presence of serum, 3 of the relatively larger LNPs (1%, 1.25% and 1.5%PEG, corresponding to 67.1, 57.3 and 53.8 nm in diameter) showed high and similar gene

silencing efficiencies (Figure 3A). On the other hand, the gene silencing activity of the smaller LNPs (2% and 3%PEG, corresponding to 45.2 and 37.3 nm in diameter) significantly decreased in response to the decreased particle size (Figure 3A). In particular, the 3%PEG-LNPs showed a low gene silencing even at the highest concentration (50 nM). These findings indicate that the lower limit of particle size for efficient gene silencing was approximately 50 nm. In contrast, in the absence of serum, the 5 kinds of LNPs induced a similar gene silencing efficiency that was independent of particle size (Figure 3B). This result also indicates that differences in the amount of PEG (1 to 3 mol%) between 5 kinds of the LNPs have a negligible effect on the gene silencing activity of the particles. In this experimental condition, no or only mild cytotoxicity was observed (Figure S2). To eliminate the possibility that this phenomenon is due to experimental conditions, we confirmed that a similar result was found in a different cell line and involving a different target gene (Figure S3).

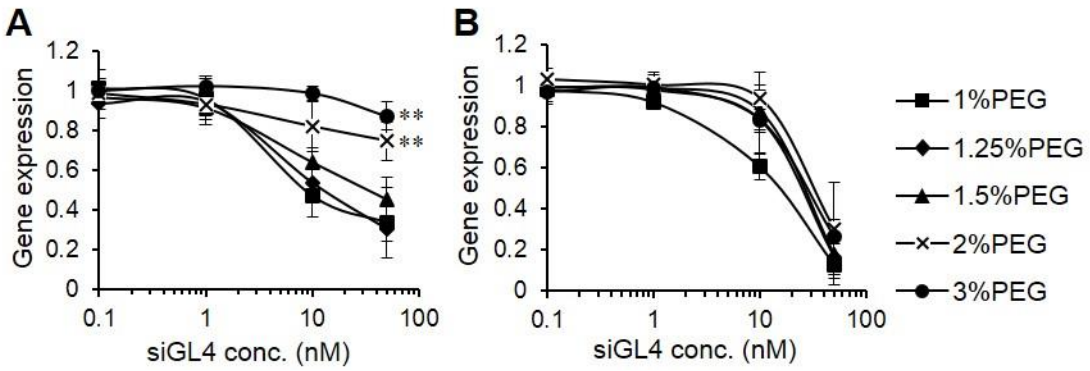

Figure 3. *In vitro* activity of the LNPs. HeLa-dluc cells were transfected with the LNPs containing different amount of PEG-DMG in the presence of serum (A) or in the absence of serum (B). Data are represented as the mean±SD. n=3-6. ***P*<0.01 (by one-way ANOVA, followed by Dunnett test, vs. 1%PEG-LNPs).

To clarify the impact of serum on the entirety of the LNPs, a cellular uptake experiment was carried out using dual-labeled LNPs with DiO and Cy5 for lipids and siRNAs, respectively. The uptake of siRNA, which was normalized by the lipid uptake, of 1%PEG-LNPs was similar in both the presence and absence of serum, indicating that the entirety of the 1%PEG-LNPs was maintained in the presence of serum (Figure 4A). A decreased siRNA uptake depending on incubation time would result from the degradation or efflux of Cy5. For the case of the 3%PEG-LNPs, in the absence of serum, the relative level of uptake of siRNA was slightly lower but similar to that of 1%PEG-LNPs. However, in the presence of serum, the relative siRNA uptake of

3%PEG-LNPs was clearly lower than the other conditions. Moreover, correlation coefficient (R) of each sample was calculated from DiO/Cy5 dot-plots (Figure S4). If most of the siRNAs were taken up as the encapsulated form, the R value would be expected to be high. On the other hand, if siRNAs leaked from the LNPs and were associated with cell membranes, which is unrelated to the uptake of the LNP lipid, the R value should be expected to be low. As shown in Figure 4B, the R value of the 1%PEG-LNPs in both conditions and the 3%PEG-LNPs in the absence of serum were approximately 0.9, which was clearly higher than that for the 3%PEG-LNPs in the presence of serum (R: 0.5 to 0.6). In addition, the leakage of siRNA in the presence of serum was detected by the cancellation of siRNA FRET. Both Cy3-labeled siRNAs and Cy5-labeled siRNAs were encapsulated in each LNP. Within each LNP, both Cy3-labeled siRNAs and Cy5-labeled siRNAs are distributed randomly and are in close proximity to each other, resulting in a reduced Cy3 fluorescence by FRET. An increase in Cy3 fluorescence (decrease in FRET efficiency) corresponds to an increased distance between neighboring siRNAs, resulting from the release of siRNAs through the destabilization of the LNPs [19, 20]. The percentage of FRET cancellation for the 3%PEG-LNPs reached 60% within 10 min, indicating that the 3%PEG-LNPs have a low stability in the presence of serum (Figure 4C). On the other hand, the 1%PEG-LNPs showed a relatively higher stability, with only a 15% decrease in FRET efficiency. Taken together with these *in vitro* experiments, it can be concluded that the smaller LNPs are destabilized by serum components and release the siRNAs before cellular uptake. This phenomenon is one possible explanation for the lower gene silencing activity of these particles. The size of the LNPs was measured after adding serum, and no significant change in the size distribution of the LNPs was observed even 30 minutes after incubation in 10% serum (Figure S5), suggesting that it would be difficult to judge the stability of the LNPs in the presence of serum by measuring particle size.

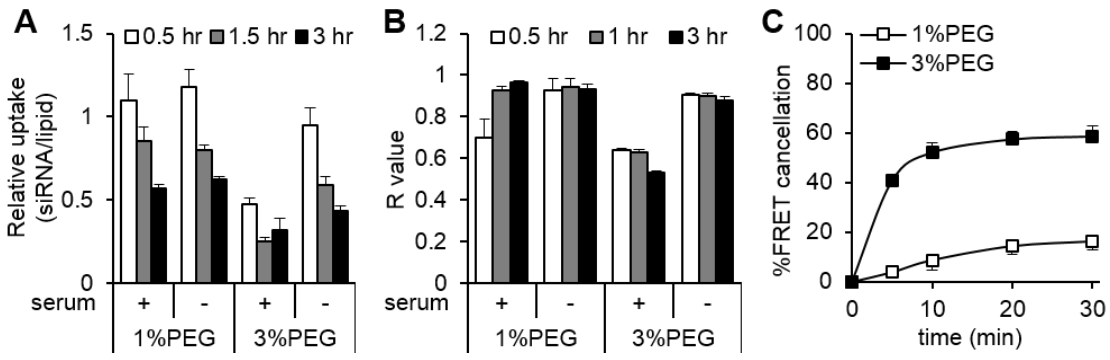

Figure 4. Evaluation of the stability of the LNPs. (A) Flow cytometric analysis of cellular uptake of dual-labeled LNPs. Data are represented as the relative siRNA uptake normalized by lipid uptake. n=4. (B) R values calculated from dot-plots of Cy5-siRNA and DiO shown in Figure S2. n=4. (C) Cancellation of siRNA FRET of the LNPs in serum. n=3. Data are represented as the mean±SD.

3.4 Investigation of lipid packing and ease of endosomal escape

To reveal the cause for reduced stability of the small-sized LNPs, the state of the particle surface was evaluated. First, the relative total surface area of the LNPs was measured. The particle sizes of the LNPs used in this assay were 55.4±2.9 nm for 1%PEG-LNPs and 32.3±3.3 nm for 3%PEG-LNPs. The total surface area of the LNPs theoretically increases in inverse proportion to particle size. Therefore, the relative total surface area of the 3%PEG-LNPs is 1.72-fold higher than that of 1%PEG-LNPs in theoretical calculations (Figure 5A). The relative total surface area can be measured by means of a fluorescent probe, TNS, as the TNS can associates with lipid membrane through hydrophobic interaction and emits strong fluorescence [21]. To avoid interactions between negatively charged TNS and positively charged YSK05, the LNPs were mixed with TNS at pH 8.5. We confirmed that negligible amounts of YSK05 were in the ionized form. Interestingly, the results showed that the relative total surface area of the 3%PEG-LNPs was 2.99-fold higher than that of the 1%PEG-LNPs (Figure 5B). Next, to measure the hydration level of the surface of the LNPs, an approach for determining changes in the generalized polarization (GP) of laurdan was carried out. The GP value depends on changes in the hydration level of the hydrophilic region of the lipid layer. A lower GP value indicates a higher hydration level on the surface of the lipid layer [22]. The GP value of the 3%PEG-LNPs was significantly lower than that of the 1%PEG-DMG, indicating that the surface of the smaller LNPs are highly hydrated (Figure 5C).

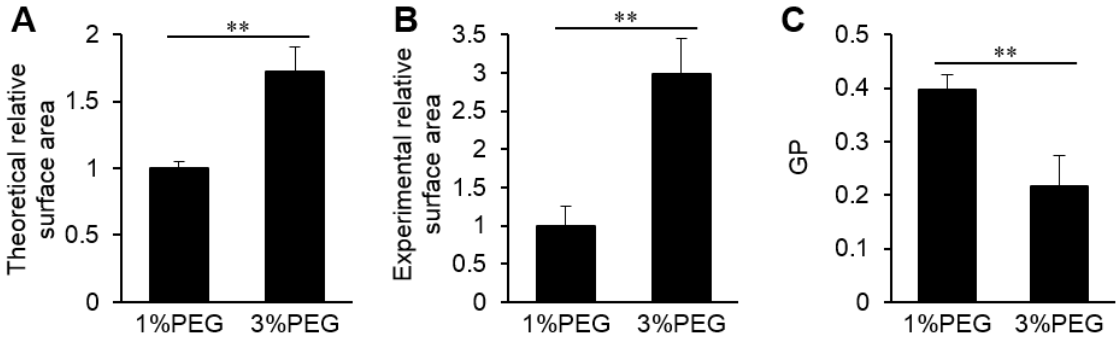

Figure 5. Evaluation of surface properties of the LNPs. (A) Theoretical relative total surface area of the LNPs calculated from the size of the LNPs measured by dynamic light scattering. n=3. (B) Experimental relative total surface area of the LNPs measured by using a fluorescent probe TNS. n=3. (C) Laurdan generalized polarization (GP) value of the LNPs. n=3. Data are represented as the mean±SD. ***P*<0.01.

As shown in Figure 3, serum significantly interfered with the integrity of the 3%PEG-LNPs and caused the release of siRNAs into media before cellular uptake. As the total surface area of the smaller LNPs are much higher than that of larger counterparts (Figure 5A, B), it is likely that the smaller LNPs are associated with higher amounts of serum components. Because the encapsulated siRNAs can be delivered to the cytosol through direct interaction and fusion between the LNP lipids and endosomal membranes, high amounts of serum components on the surface of the LNPs would suppress the extent of interaction and fusion. Zhang Y et al. recently reported on the development of an *in vitro* assay to evaluate the efficiency of siRNA release to cytosol [23]. This assay mimics the conditions for the release of siRNA by means of interactions of lipid nanoparticles with serum followed by a decrease in pH and the interaction with endosome-mimicking negatively charged liposomes. The efficiency of siRNA release in this assay was in good agreement with the *in vivo* gene silencing activity in hepatocytes. We carried out this assay to compare the siRNA release efficiency between 1%PEG-LNPs and 3%PEG-LNPs. As shown in Figure 6A, the percentage of siRNA release on the 1%PEG-LNPs was significantly higher than that on the 3%PEG-LNPs. This result indicates that serum has a measurable impact on the process of the endosomal escape. Furthermore, a hemolysis assay is frequently used to evaluate the membrane disruption activity of nucleic acid delivery carriers. The hemolytic activity of the 1%PEG-LNPs and 3%PEG-LNPs was measured in the presence of serum in order to evaluate the influence of serum on endosomal escape. As shown in Figure 6B, the hemolytic activity of the both LNPs significantly decreased with increasing amounts of serum protein. However, the inhibitory effect on 3%PEG-LNPs was significantly higher than that of the 1%PEG-LNPs. This result suggests that the process of endosomal escape of the smaller LNPs can be highly inhibited by serum components compared to the larger counterparts. These collective results clarify that the efficiency of siRNA delivery for the smaller LNPs was decreased through not only enhanced siRNA release before cellular uptake but also by a reduced efficiency of endosomal escape.

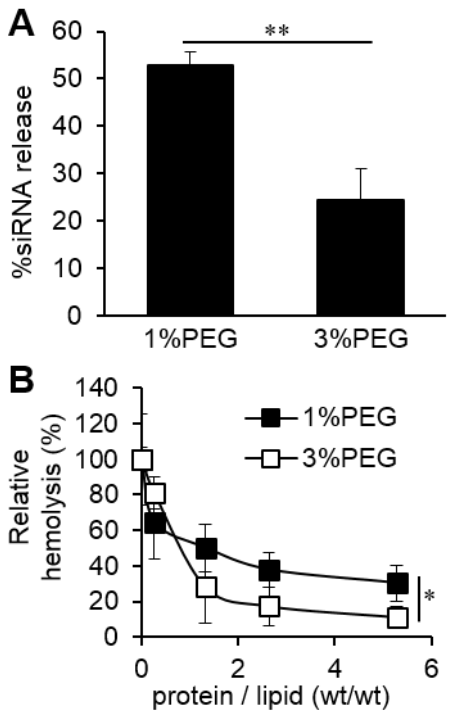

Figure 6. Evaluation of potency for endosomal escape of the LNPs. (A) Activity of cytosolic siRNA release. n=3. (B) Hemolytic activity of the LNPs in the presence of serum. n=3. Data are represented as the mean±SD. *P<0.05, **P<0.01.

3.5 Significance of endosomal escape process

We next attempted to clarify the impact of inhibiting endosomal escape for the small-sized LNPs. Cholesterol is known to increase the packing of lipids with unsaturated carbon chains [24]. Therefore, to stabilize LNPs and avoid siRNA leakage in the blood circulation, the proportion of cholesterol in the PEG-LNPs was increased from 30 to 50 mol%. The diameters of the 1%PEG-LNPs and 3%PEG-LNPs containing 50 mol% cholesterol were 47.0 nm and 31.3 nm, slightly smaller than each counterpart containing 30% cholesterol in their lipid composition. A FRET assay confirmed that the cholesterol-rich 3%PEG-LNPs showed a similar rate of siRNA leakage as 1%PEG-LNPs containing 30 mol% of cholesterol (Figure 4C and Figure S6A), indicating that the stability of small-sized LNPs in the blood circulation was increased by increased amount of cholesterol. The results of a cellular uptake study also supported the conclusion that the stability of the 3%PEG-LNPs was enhanced by an increase in cholesterol content (Figure S6B). Taken together, cholesterol-rich LNPs can be used to

investigate the inhibitory impact of the endosomal escape process on small-sized LNPs without significant leakage of siRNAs from the LNPs in the blood circulation. To confirm whether cholesterol-rich 3%PEG-LNPs efficiently deliver siRNAs to hepatocytes, liver tissues were observed after intravenous injection of Cy5-labeled siRNA-loaded 1%PEG-LNPs and 3%PEG-LNPs, which contain 50 mol% cholesterol in their lipid composition. As shown in Figure 7A, different from Figure 2C, the amounts of siRNAs delivered by the 3%PEG-LNPs was similar to that for the 1%PEG-LNPs. On the other hand, similar to Figure 2C, the hepatocellular siRNA localization of the 1%PEG-LNPs and 3%PEG-LNPs showed a diffuse pattern and a punctuate pattern, respectively. Finally, the FVII gene silencing activity of the two cholesterol-rich LNPs was examined. Despite similar levels of siRNAs delivered to hepatocytes, it was observed that the activity of the 3%PEG-LNPs was significantly lower than that of the 1%PEG-LNPs (Figure 7B).

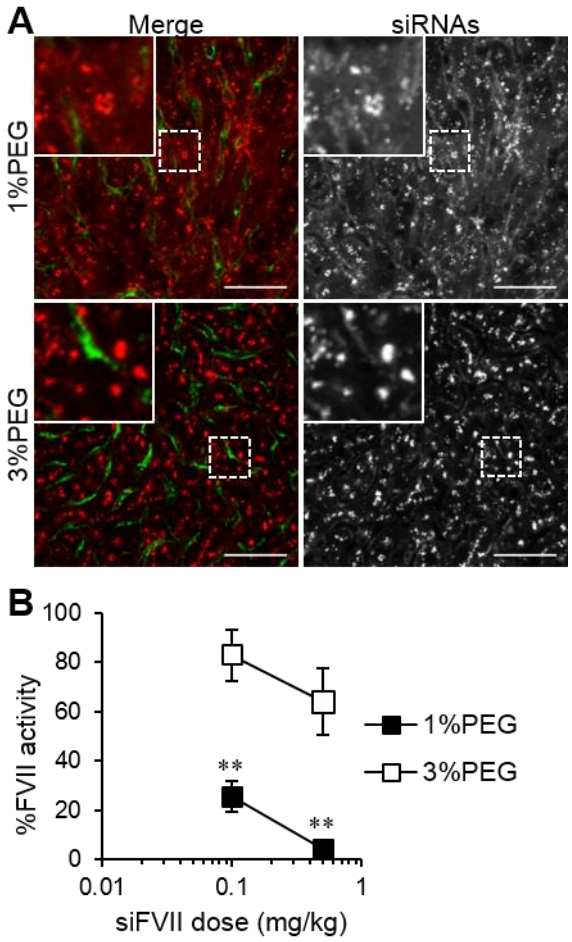

Figure 7. *In vivo* activity and biodistribution of the cholesteol-rich LNPs. (A) Intrahepatic distribution of siRNAs delivered by the LNPs. Blood vessels and

siRNAs are visualized as green and red, respectively. Scale bars indicate 50 μm. (B) FVII gene silencing activity of the LNPs. n=3. Data are represented as the mean±SD. **P<0.01.

Discussion

Since small-sized nanoparticles with diameters less than 50 nm can penetrate stromal-rich tumor tissues [8, 12], highly potent and small-sized siRNA-loaded nanoparticles are promising candidates for achieving effective RNAi-based cancer therapy. LNPs are the leading systems for *in vivo* delivery of siRNAs. However, although small-sized LNPs have recently been synthesized by a microfluidic mixing technique [14, 16, 17], their physicochemical properties and potency for siRNA delivery have not been fully characterized. Therefore, in the present study, we characterized the potency of small-sized LNPs for *in vivo* siRNA delivery. A summary of the findings in the present study is shown in Figure 8.

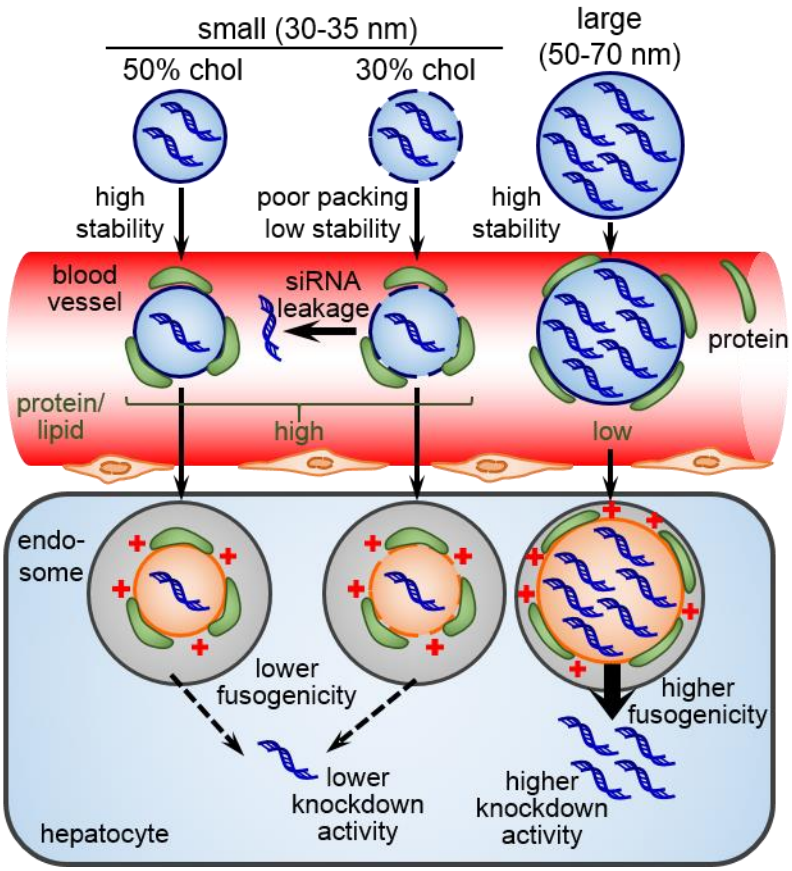

Figure 8. Schematic illustration of the findings in the present study. Poor lipid packing of 30% cholesterol containing small-sized LNPs results in siRNA leakage after absorption of serum proteins. Large-sized LNPs show higher

endosomal escape potency because of lower adsorption of serum proteins per lipid. On the other hand, higher protein absorption per lipid of the small-sized LNPs cause severe inhibition of the endosomal escape process, resulting in lower knockdown activity.

The apparent pKa value, which is critical factor for the biodistribution and gene silencing activity of siRNA-loaded LNPs, of the 3%PEG-LNPs was slightly higher than that of the 1%PEG-LNPs (6.45 vs. 6.25). However, as it has been reported that the optimal pKa value for hepatocellular siRNA delivery is the range from 6.2 to 6.5 [1], this difference would not be a key factor in explaining the significant difference in the potency for siRNA delivery between the two LNPs.

The leakage of siRNAs from the 3%PEG-LNPs was observed both *in vivo* and *in vitro*. However, no significant leakage of siRNAs was observed in the absence of serum *in vitro*, indicating that the adsorption of serum components destabilized the 3%PEG-LNPs. Based on the results of GP measurements, the 3%PEG-LNPs were more hydrated than the 1%PEG-LNPs (Figure 5C). It is possible that a higher amount of PEG-DMG would increase the degree of hydration of the surface of the LNPs and decrease the GP value [25]. As shown in Figure 5B, the actual (experimentally calculated) relative total surface area of the 3%PEG-LNPs was 2.99-fold higher than that of 1%PEG-LNPs. Therefore, the density of the PEG-DMG, which is equal to the number of the PEG-DMG per unit area, is similar between the two types of LNPs. Therefore, such a scenario can be ignored in this case. As the particle size decrease, the curvature of the surface of the particles becomes larger. On the other hand, a main component of the LNPs, YSK05, has a cone-shaped structure, and the aggregate of the YSK05 has a tendency to form an inverted hexagonal phase, which has a highly negative curvature. Therefore, the emphasized strain between the real curvature of the surface of the small-sized 3%PEG-LNPs and the spontaneous curvature of the YSK05 aggregates would cause the distances between lipids on the surface of the small-sized LNPs to be widened, resulting in a higher hydration, a lower lipid packing and a decreased physical stability. Moreover, as shown in Figures 5A and 5B, the experimentally determined relative total surface area of the 3%PEG-LNPs (2.99) was higher than the theoretical relative total surface area of the same LNPs (1.72). The theoretical surface area is a predicted value determined by a simple calculation using the formula described in Materials and methods. Therefore, a change in lipid-packing is not considered in the theoretical value. On the other hand, the experimental surface area directly reflects the amount of TNS interacting with the particle surface, which is an

indicator of the actual total surface area. Therefore, an extra relative total surface area of the 3%PEG-LNPs supports poor lipid-packing. PEG-DMG contributes to the colloidal stability of the 3%PEG-LNPs when suspended in a buffer. However, the PEG-DMG is known to rapidly diffuse from the surface of the LNPs in the presence of serum [26]. Taken together, poor lipid packing and the diffusion of the PEG-DMG appears to result in the significant destabilization and siRNA leakage in the case of the 3%PEG-LNPs.

As the relative total surface area of the 3%PEG-LNPs was 3-fold higher than that of the 1%PEG-LNPs, the amount of protein adsorbed to the surface of the 3%PEG-LNPs would be expected to be high. A higher amount of protein on the surface of the LNPs inhibits their potency for endosomal escape because endosomal escape can be achieved through a direct interaction between cationic lipids of the LNPs and anionic lipids on the endosomal membrane, followed by membrane fusion. We attempted to compare the amount of the protein adsorbed to both LNPs, but failed, possibly because their small size (near the sizes of lipoproteins) and low stability during the separation of the protein adsorbed LNPs from free proteins. However, we detected a significant difference in potency for endosomal escape between the 1%PEG-LNPs and the 3%PEG-LNPs. As shown in Figure 6B, the higher inhibitory effect of plasma proteins on hemolytic activity of the 3%PEG-LNPs suggests that a higher amount of proteins are absorbed to the same LNPs. The lower membrane fusion activity of the 3%PEG-LNPs resulted in a reduced potency for the cytosolic release of siRNAs (Figure 6A). Moreover, we found that siRNAs delivered by the 3%PEG-LNPs showed a punctuate pattern rather than a diffuse pattern (Fig. 2C, 7A). This observation reflects the lower endosomal escape for the 3%PEG-LNPs. Although it is recognized that the detection of the diffused siRNAs in the cytosol is difficult by using a typical confocal laser scanning microscopic system because of the low signal/noise ratio [27, 28], previous reports succeeded in detecting cytosolic siRNAs under conditions where the siRNA dose was much higher than the ED_{50} value [15, 29]. Therefore, in this study, for the observation of intrahepatic siRNA localization, a higher siRNA dose (0.5 mg/kg) was used in detecting the diffused siRNAs in the cytosol. Indeed, the diffused siRNAs in cytosol could be detected in liver tissue only in the case of the administration of the 1%PEG-LNPs, which induced more than 90% gene silencing at the same dose, but not the 3%PEG-LNPs, which showed lower activity (Figure 2C, 7A).

To clarify the impact of the reduced potency for endosomal escape on the small-sized LNPs, the proportion of cholesterol in the LNP composition was increased from 30 mol% to 50 mol% in order to enhance the physical stability and minimize the leakage of siRNA in the blood circulation. In spite of the efficient delivery of siRNA to

hepatocytes (Figure 7A), the cholesterol-rich 3%PEG-LNPs showed a significantly lower gene silencing activity compared to the larger counterparts (Figure 7B), which strongly suggests that the reduced potency for endosomal escape is caused by higher amounts of adsorbed proteins, which substantially contribute to the reduced gene silencing activity.

The findings reported herein clarify that the absorption of high amounts of protein to the particles are the fundamental cause for the reduction in gene silencing activity for the small-sized LNPs. Therefore, it would be expected that the inhibition of the protein adsorption represents a potentially effective strategy for developing highly potent, small-sized LNPs. It is generally accepted that the PEGylation of nanoparticles involves the formation of a thick hydrated layer on their surface [30] and that this efficiently minimizes protein adsorption [31, 32]. Therefore, we prepared small-sized LNPs modified with 3 mol% of PEG-distearoylglycerol (DSG), which diffuses from the LNPs with difficulty [26], instead of PEG-DMG, but the leakage of siRNAs was not reduced by the PEG-DSG modification (data not shown). It is possible that the density of the PEG-DSG on the surface of the LNPs was insufficient to suppress protein adsorption. However, the insertion of a higher amount of PEG-DSG would result in the ‘PEG-dilemma’ [33, 34], which leads to the enhanced stability of LNPs but strongly reduces the potency for endosomal escape because the thick PEG layer physically inhibits membrane interactions. Therefore, optimization of the length and density of the PEG or rational environment-responsive technologies will be necessary to overcome such a severe problem and to develop next-generation highly potent, small-sized LNPs.

Conclusion

Small-sized siRNA-loaded LNPs are promising platforms for novel RNAi-based cancer therapy because of their superior ability to penetrate into tumor tissues. In the present study, we investigated the effect of the downsizing LNPs on their physicochemical properties and potency for delivering siRNAs. We found that small-sized LNPs showed a reduced lipid packing, reduced stability and a reduced ability for endosomal escape, and the fundamental cause appears to a higher amount protein being adsorbed on the surface of the LNPs. Inhibiting such protein adsorption would be a particularly useful strategy for the development of the highly potent, small-sized LNPs. We believe that the findings reported in this communication will contribute to the development of the next generation RNAi-based nanomedicines.

Acknowledgement

This work was supported by JSPS KAKENHI Grant Number 15K20831. The authors also wish to thank Dr. Milton S. Feather for his helpful advice in writing the English manuscript.

References

[1] M. Jayaraman, S.M. Ansell, B.L. Mui, Y.K. Tam, J. Chen, X. Du, D. Butler, L. Eltepu, S. Matsuda, J.K. Narayanannair, K.G. Rajeev, I.M. Hafez, A. Akinc, M.A. Maier, M.A. Tracy, P.R. Cullis, T.D. Madden, M. Manoharan, M.J. Hope, Maximizing the potency of siRNA lipid nanoparticles for hepatic gene silencing in vivo, Angew Chem Int Ed Engl, 51 (2012) 8529-8533.

[2] C.I. Wooddell, D.B. Rozema, M. Hossbach, M. John, H.L. Hamilton, Q. Chu, J.O. Hegge, J.J. Klein, D.H. Wakefield, C.E. Oropeza, J. Deckert, I. Roehl, K. Jahn-Hofmann, P. Hadwiger, H.P. Vornlocher, A. McLachlan, D.L. Lewis, Hepatocyte-targeted RNAi therapeutics for the treatment of chronic hepatitis B virus infection, Mol Ther, 21 (2013) 973-985.

[3] J.K. Nair, J.L. Willoughby, A. Chan, K. Charisse, M.R. Alam, Q. Wang, M. Hoekstra, P. Kandasamy, A.V. Kel'in, S. Milstein, N. Taneja, J. O'Shea, S. Shaikh, L. Zhang, R.J. van der Sluis, M.E. Jung, A. Akinc, R. Hutabarat, S. Kuchimanchi, K. Fitzgerald, T. Zimmermann, T.J. van Berkel, M.A. Maier, K.G. Rajeev, M. Manoharan, Multivalent N-acetylgalactosamine-conjugated siRNA localizes in hepatocytes and elicits robust RNAi-mediated gene silencing, J Am Chem Soc, 136 (2014) 16958-16961.

[4] Y. Matsumura, H. Maeda, A new concept for macromolecular therapeutics in cancer chemotherapy: mechanism of tumoritropic accumulation of proteins and the antitumor agent smancs, Cancer Res, 46 (1986) 6387-6392.

[5] H. Maeda, T. Sawa, T. Konno, Mechanism of tumor-targeted delivery of macromolecular drugs, including the EPR effect in solid tumor and clinical overview of the prototype polymeric drug SMANCS, J Control Release, 74 (2001) 47-61.

[6] C.K. Anders, B. Adamo, O. Karginova, A.M. Deal, S. Rawal, D. Darr, A. Schorzman, C. Santos, R. Bash, T. Kafri, L. Carey, C.R. Miller, C.M. Perou, N. Sharpless, W.C. Zamboni, Pharmacokinetics and efficacy of PEGylated liposomal doxorubicin in an intracranial model of breast cancer, PLoS One, 8 (2013) e61359.

[7] L. Eikenes, M. Tari, I. Tufto, O.S. Bruland, C. de Lange Davies, Hyaluronidase induces a transcapillary pressure gradient and improves the distribution and uptake of liposomal doxorubicin (Caelyx) in human osteosarcoma xenografts, Br J Cancer, 93 (2005) 81-88.

[8] H. Cabral, J. Makino, Y. Matsumoto, P. Mi, H. Wu, T. Nomoto, K. Toh, N. Yamada, Y. Higuchi, S. Konishi, M.R. Kano, H. Nishihara, Y. Miura, N. Nishiyama, K. Kataoka, Systemic Targeting of Lymph Node Metastasis through the Blood Vascular System by Using Size-Controlled Nanocarriers, ACS Nano, 9 (2015) 4957-4967.

[9] V.P. Chauhan, R.K. Jain, Strategies for advancing cancer nanomedicine, Nat Mater, 12 (2013) 958-962.

[10] P.A. Netti, D.A. Berk, M.A. Swartz, A.J. Grodzinsky, R.K. Jain, Role of extracellular matrix assembly in interstitial transport in solid tumors, Cancer Res, 60 (2000) 2497-2503.
[11] C.J. Whatcott, H. Han, R.G. Posner, G. Hostetter, D.D. Von Hoff, Targeting the tumor microenvironment in cancer: why hyaluronidase deserves a second look, Cancer Discov, 1 (2011) 291-296.
[12] H. Cabral, Y. Matsumoto, K. Mizuno, Q. Chen, M. Murakami, M. Kimura, Y. Terada, M.R. Kano, K. Miyazono, M. Uesaka, N. Nishiyama, K. Kataoka, Accumulation of sub-100 nm polymeric micelles in poorly permeable tumours depends on size, Nat Nanotechnol, 6 (2011) 815-823.
[13] I.V. Zhigaltsev, N. Belliveau, I. Hafez, A.K. Leung, J. Huft, C. Hansen, P.R. Cullis, Bottom-up design and synthesis of limit size lipid nanoparticle systems with aqueous and triglyceride cores using millisecond microfluidic mixing, Langmuir, 28 (2012) 3633-3640.
[14] N.M. Belliveau, J. Huft, P.J. Lin, S. Chen, A.K. Leung, T.J. Leaver, A.W. Wild, J.B. Lee, R.J. Taylor, Y.K. Tam, C.L. Hansen, P.R. Cullis, Microfluidic Synthesis of Highly Potent Limit-size Lipid Nanoparticles for In Vivo Delivery of siRNA, Mol Ther Nucleic Acids, 1 (2012) e37.
[15] Y. Sato, H. Hatakeyama, Y. Sakurai, M. Hyodo, H. Akita, H. Harashima, A pH-sensitive cationic lipid facilitates the delivery of liposomal siRNA and gene silencing activity in vitro and in vivo, J Control Release, 163 (2012) 267-276.
[16] A.K. Leung, I.M. Hafez, S. Baoukina, N.M. Belliveau, I.V. Zhigaltsev, E. Afshinmanesh, D.P. Tieleman, C.L. Hansen, M.J. Hope, P.R. Cullis, Lipid Nanoparticles Containing siRNA Synthesized by Microfluidic Mixing Exhibit an Electron-Dense Nanostructured Core, J Phys Chem C Nanomater Interfaces, 116 (2012) 18440-18450.
[17] A.K. Leung, Y.Y. Tam, S. Chen, I.M. Hafez, P.R. Cullis, Microfluidic Mixing: A General Method for Encapsulating Macromolecules in Lipid Nanoparticle Systems, J Phys Chem B, 119 (2015) 8698-8706.
[18] T. Watanabe, H. Hatakeyama, C. Matsuda-Yasui, Y. Sato, M. Sudoh, A. Takagi, Y. Hirata, T. Ohtsuki, M. Arai, K. Inoue, H. Harashima, M. Kohara, In vivo therapeutic potential of Dicer-hunting siRNAs targeting infectious hepatitis C virus, Sci Rep, 4 (2014) 4750.
[19] K.A. Whitehead, G. Sahay, G.Z. Li, K.T. Love, C.A. Alabi, M. Ma, C. Zurenko, W. Querbes, R.S. Langer, D.G. Anderson, Synergistic silencing: combinations of lipid-like materials for efficacious siRNA delivery, Mol Ther, 19 (2011) 1688-1694.
[20] C.A. Alabi, K.T. Love, G. Sahay, T. Stutzman, W.T. Young, R. Langer, D.G. Anderson, FRET-labeled siRNA probes for tracking assembly and disassembly of siRNA nanocomplexes, ACS Nano, 6 (2012) 6133-6141.

[21] K. Sou, T. Endo, S. Takeoka, E. Tsuchida, Poly(ethylene glycol)-modification of the phospholipid vesicles by using the spontaneous incorporation of poly(ethylene glycol)-lipid into the vesicles, Bioconjug Chem, 11 (2000) 372-379.
[22] T. Parasassi, G. De Stasio, G. Ravagnan, R.M. Rusch, E. Gratton, Quantitation of lipid phases in phospholipid vesicles by the generalized polarization of Laurdan fluorescence, Biophys J, 60 (1991) 179-189.
[23] Y. Zhang, L. Arrington, D. Boardman, J. Davis, Y. Xu, K. DiFelice, S. Stirdivant, W. Wang, B. Budzik, J. Bawiec, J. Deng, G. Beutner, D. Seifried, M. Stanton, M. Gindy, A. Leone, The development of an in vitro assay to screen lipid based nanoparticles for siRNA delivery, J Control Release, 174 (2014) 7-14.
[24] W.C. Hung, M.T. Lee, F.Y. Chen, H.W. Huang, The condensing effect of cholesterol in lipid bilayers, Biophys J, 92 (2007) 3960-3967.
[25] Y. Maitani, A. Nakamura, T. Tanaka, Y. Aso, Hydration of surfactant-modified and PEGylated cationic cholesterol-based liposomes and corresponding lipoplexes by monitoring a fluorescent probe and the dielectric relaxation time, Int J Pharm, 427 (2012) 372-378.
[26] B.L. Mui, Y.K. Tam, M. Jayaraman, S.M. Ansell, X. Du, Y.Y. Tam, P.J. Lin, S. Chen, J.K. Narayanannair, K.G. Rajeev, M. Manoharan, A. Akinc, M.A. Maier, P. Cullis, T.D. Madden, M.J. Hope, Influence of Polyethylene Glycol Lipid Desorption Rates on Pharmacokinetics and Pharmacodynamics of siRNA Lipid Nanoparticles, Mol Ther Nucleic Acids, 2 (2013) e139.
[27] J. Gilleron, W. Querbes, A. Zeigerer, A. Borodovsky, G. Marsico, U. Schubert, K. Manygoats, S. Seifert, C. Andree, M. Stöter, H. Epstein-Barash, L. Zhang, V. Koteliansky, K. Fitzgerald, E. Fava, M. Bickle, Y. Kalaidzidis, A. Akinc, M. Maier, M. Zerial, Image-based analysis of lipid nanoparticle-mediated siRNA delivery, intracellular trafficking and endosomal escape, Nat Biotechnol, 31 (2013) 638-646.
[28] A. Wittrup, A. Ai, X. Liu, P. Hamar, R. Trifonova, K. Charisse, M. Manoharan, T. Kirchhausen, J. Lieberman, Visualizing lipid-formulated siRNA release from endosomes and target gene knockdown, Nat Biotechnol, 33 (2015) 870-876.
[29] G. Basha, T.I. Novobrantseva, N. Rosin, Y.Y. Tam, I.M. Hafez, M.K. Wong, T. Sugo, V.M. Ruda, J. Qin, B. Klebanov, M. Ciufolini, A. Akinc, Y.K. Tam, M.J. Hope, P.R. Cullis, Influence of cationic lipid composition on gene silencing properties of lipid nanoparticle formulations of siRNA in antigen-presenting cells, Mol Ther, 19 (2011) 2186-2200.
[30] I. Sugiyama, T. Sonobe, Y. Sadzuka, Effect of hybridized liposome by novel modification with some polyethyleneglycol-lipids, Int J Pharm, 372 (2009) 177-183.
[31] P.R. Cullis, A. Chonn, S.C. Semple, Interactions of liposomes and lipid-based carrier systems with blood proteins: Relation to clearance behaviour in vivo, Adv Drug Deliv Rev, 32

(1998) 3-17.
[32] N. Dos Santos, C. Allen, A.M. Doppen, M. Anantha, K.A. Cox, R.C. Gallagher, G. Karlsson, K. Edwards, G. Kenner, L. Samuels, M.S. Webb, M.B. Bally, Influence of poly(ethylene glycol) grafting density and polymer length on liposomes: relating plasma circulation lifetimes to protein binding, Biochim Biophys Acta, 1768 (2007) 1367-1377.
[33] H. Hatakeyama, H. Akita, H. Harashima, The polyethyleneglycol dilemma: advantage and disadvantage of PEGylation of liposomes for systemic genes and nucleic acids delivery to tumors, Biol Pharm Bull, 36 (2013) 892-899.
[34] H. Hatakeyama, H. Akita, H. Harashima, A multifunctional envelope type nano device (MEND) for gene delivery to tumours based on the EPR effect: a strategy for overcoming the PEG dilemma, Adv Drug Deliv Rev, 63 (2011) 152-160.